

# Fairness-Optimized Synthetic EHR Generation for Arbitrary Downstream Predictive Tasks

Mirza Farhan Bin Tarek, Raphael Poulain, Rahmatollah Beheshti

University of Delaware  
{mfarhan, rpoulain, rbi}@udel.edu

## Abstract

Among various aspects of ensuring the responsible design of AI tools for healthcare applications, addressing fairness concerns has been a key focus area. Specifically, given the wide spread of electronic health record (EHR) data and their huge potential to inform a wide range of clinical decision support tasks, improving fairness in this category of health AI tools is of key importance. While such a broad problem (that is, mitigating fairness in EHR-based AI models) has been tackled using various methods, task- and model-agnostic methods are noticeably rare. In this study, we aimed to target this gap by presenting a new pipeline that generates synthetic EHR data, which is not only consistent with (faithful to) the real EHR data but also can reduce the fairness concerns (defined by the end-user) in the downstream tasks, when combined with the real data. We demonstrate the effectiveness of our proposed pipeline across various downstream tasks and two different EHR datasets. Our proposed pipeline can add a widely applicable and complementary tool to the existing toolbox of methods to address fairness in health AI applications such as those modifying the design of a downstream model<sup>1</sup>.

## Introduction

The integration of ML and AI into healthcare has become increasingly feasible with the widespread adoption of EHR systems. EHRs are complex, encompassing several thousand distinct medical codes related to diagnoses, procedures, medications, and lab measurements, resulting in intricate relationships and patterns among these codes. Different ML models are helping in different aspects of healthcare, for example, clinical predictive modeling (Choi et al. 2016, 2017a; Ramazi et al. 2019; Gupta et al. 2022), computational phenotyping (Che and Liu 2017; Fu et al. 2019), subtyping patients (Mottalib et al. 2023) and treatment suggestions (Wang et al. 2018; Shang et al. 2019a,b). However, privacy laws, such as the Health Insurance Portability and Accountability Act (HIPAA) (Moore and Frye 2020) in the United States and the General Data Protection Regulation (GDPR) in the European Union (Voigt and von dem Bussche 2017) create restrictions in accessing EHRs, posing difficulty in

reproducibility and limiting the scope of research endeavors. Synthetic data can enable researchers to work with more data when the amount of real data is limited. Especially in the healthcare domain, it is essential for synthetic data to faithfully represent real data, ensuring accuracy, and fairness while safeguarding patient privacy. This ensures that analyses conducted on synthetic data can be replicated on real data. The utility of synthetic data is gauged by the performance of ML models generated on it, aiming for similarity to models trained on real data. It thus should mirror the characteristics of the real data, exhibiting similar utility and fairness, even in the presence of biases. This means the generated data should have comparable or better performance in downstream prediction tasks (e.g., the popular patient mortality prediction task) and the prediction should be devoid of any bias (Bhanot et al. 2022).

While synthetic data generation is valuable, it does not comprehensively address all challenges. Real data inherently carries biases that can manifest in various forms, affecting demographic, behavioral, textual, and visual data. If the downstream model is trained on biased real or synthetic data, that bias would be transferred to the model resulting in biased outputs. This can lead to discrimination and unfair treatment of individuals (Xu et al. 2018). That is why we have developed an end-to-end pipeline incorporating a fairness-optimized synthetic EHR data generator to create a large dataset and reduce the bias in the downstream tasks. During data generation, the pipeline can output fairness-optimized augmented data by utilizing a fairness optimization (FO) objective. To our knowledge, this is the first of its kind. Our key contributions are:

- **Implement a FO objective function in a synthetic EHR data generation process.** We have implemented a metric-agnostic fairness optimization objective in the training process of a synthetic EHR generator to optimize the generated data for fairness.
- **Integrate the fairness-optimized generator into a pipeline to output augmented data for less-biased downstream task outputs.** Our proposed pipeline aims to make the output of downstream tasks less biased by augmenting real EHR data with the FO synthetic data.

Copyright © 2024, Association for the Advancement of Artificial Intelligence (www.aaai.org). All rights reserved.

<sup>1</sup>The codebase for our project is available at <https://github.com/healthyiaife/FairSynth>

## Related Work

### Fairness in Machine Learning

Fairness within ML can be viewed in various ways. One common way relates to categorizing fairness into two primary types: (i) group fairness (Chouldechova and Roth 2018), and (ii) individual fairness (Dwork et al. 2012). Our focus in this research is primarily on group fairness, which involves assessing the discrepancy in performance across the groups (including the protected and privileged groups). This emphasis aims to highlight systemic biases against specific groups. As defined in the literature, group fairness exhibits diverse interpretations, often selected based on stakeholders' perspectives and, at times, presenting conflicting behaviors in specific contexts (Narayanan 2018; Poulain, Bin Tarek, and Beheshti 2023).

Relatedly, a common (despite its caveats) way to categorize the methods to mitigate bias in the ML community includes (i) pre-processing techniques, which modify input data to eliminate information correlated with sensitive attributes; (ii) in-processing methods, which impose fairness constraints during the model learning process; and (iii) post-processing approaches, which adjust model predictions after training (Ras et al. 2022). In our research, we will process the data and optimize the generator model for fairness.

### Synthetic and Fair EHR Data Generation

Many approaches exist for generating synthetic EHR data. A common approach is using Generative Adversarial Networks (GANs), which are commonly used for generating images and have been used in generating EHR data with moderate success (Goodfellow et al. 2014; Choi et al. 2017b; Zhang et al. 2021; Torfi and Fox 2020; Cui et al. 2020; Baowaly et al. 2019; Sun et al. 2021). Generating sequential EHR data is challenging with GANs as they often produce individual outputs without temporal connections. To address this limitation, various strategies have been employed, such as aggregating data into one-time steps (Zhang et al. 2020; Yan et al. 2020; Rashidian et al. 2020), creating data representations (Cui et al. 2020), or combining both approaches (Choi et al. 2017b; Baowaly et al. 2019). GANs also face difficulties handling high-dimensional and sparse real-world EHR data, restricting existing synthetic EHR GAN approaches to relatively low-dimensional output by aggregating visits and medical codes or removing rare codes. For example, methods generating longitudinal data, such as `LongGAN` (Sun et al. 2021) and `EHR-M-GAN` (Li et al. 2023), focus solely on dense lab time series with dimensions under a hundred. Despite the potential of conditioning GANs on external factors and labels, such as demographics or disease phenotype labels, limited exploration of this capability exists in current works on EHR generation.

Another synthetic data generation approach is diffusion models, which have emerged as an approach for realistic synthetic data generation. Specifically, denoising diffusion probabilistic models (DDPMs) are a class of latent variable models that can learn the underlying distribution of data by transforming samples into standard Gaussian noise and

training the model to denoise these corrupted samples back to their original forms (Ceritli et al. 2023).

In addition to their stable training, DDPMs have demonstrated superior performance compared to generative adversarial networks (GANs) in generating synthetic images, audio, and tabular data (Ceritli et al. 2023). Recently, He et al. (2023) proposed `medDiff`, a DDPM specifically designed for electronic health records (EHRs), showcasing the benefits of diffusion models over existing methods. However, `medDiff` works best to generate continuous values as it employs a Gaussian diffusion process, assuming the data follows a Gaussian distribution, even though medical data often contains both continuous features (e.g., blood test results) and categorical features (e.g., sex and ethnicity). While one can round the outputs of `medDiff` to obtain discrete values, a more principled approach would be to generate categorical data directly, eliminating the need for post-processing and potentially leading to more accurate synthetic samples. Following this, Ceritli et al. (2023) proposed `TabDDPM` which is a diffusion model to generate tabular EHRs with continuous or temporal (which changes over time e.g. lab results, vital signs) and static data (which does not change over time e.g. patient gender, ethnicity, etc.). However, the author did not include the effectiveness of these methods in generating datasets that can achieve fair results in downstream tasks.

Finally, with the recent rise of large language models, researchers have already started using them for synthetic EHR data generation. Large language models utilize transformers (Vaswani et al. 2017) in their architectures and they have been used for many tasks in different domains for example in developing large language models (Devlin et al. 2018; Radford et al. 2019; Touvron et al. 2023) and in healthcare for primordial prevention (Poulain et al. 2021), few-shot learning (Poulain, Gupta, and Beheshti 2022). `HALO` or Hierarchical Autoregressive Language Model for synthetic EHR data generator can generate a probability density function over different medical codes, clinical visits, and patient records. This allows the generation of realistic EHR data (Theodorou, Xiao, and Sun 2023). In addition to autoregressive methods, GPT or Generative Pre-trained Transformer models have been used recently to generate EHR. In the work by Pang et al. (2024), the authors proposed a `CEHR-GPT` framework that treats patient generation as a language modeling problem similar to `HALO` but they have used the state-of-the-art GPT language model for the task. Furthermore, their patient representation can also preserve track of the different visit types and discharge facilities for inpatient visits in addition to preserving the temporal information.

### Problem Statement

Structured electronic health records (EHR) are multi-level longitudinal data that show each patient as a series of visits. Each visit is represented by a set of medical codes that include static patient data (e.g. demographics, disease phenotype labels, diagnoses, procedures, and medications codes), and continuous data (e.g. lab test results). In our project, we have developed a pipeline for generating

Fairness-Optimized (FO) augmented EHR data by implementing a fairness objective  $F$  in the synthetic data generator and later joining the FO synthetic data and the real data together to create an augmented dataset. Now, we establish a formal representation below:

Given a real EHR dataset  $R$ , a fairness objective function  $F$ , and a generation process function  $G$ , the goal is to generate a Fairness-Optimized (FO) synthetic EHR dataset  $R'$  and augment  $R$  with it. We represent our pipeline in as:

$$R + G(R, F) = R + R'. \quad (1)$$

We represent the fairness objective  $F$  as a loss function  $\mathcal{L}_F$ , weighted by the fairness weight  $\lambda$ , in Eq 2 that will be implemented in the generator in addition to the generator’s loss  $L(y, \hat{y})$  to calculate the total loss  $L_{model}$  to ensure that the positive outcomes (in our experiments, the outcome is binary mortality prediction) for the minority group are proportionally similar to the majority group for a certain sensitive attribute  $S \in \{[1, M]\}$ , where  $S$  is a categorical sensitive attribute with  $M$  possible values (e.g. gender, age, race, and ethnicity).

$$\mathcal{L}_{model} = \mathcal{L}(y, \hat{y}) + \lambda \mathcal{L}_F \quad (2)$$

### Pipeline Description

The pipeline mainly consists of three parts: i) data pre-processing, ii) FO synthetic data generation, and iii) data augmentation (Figure 1). In the following sections, we describe our pipeline in detail.

#### Data pre-processing

Pre-processing can include steps like filtering the data based on specific features and imputing the missing values. Here, we process the input EHR data in a format suitable for the generator  $G$ . The data  $R$  comprises  $N$  patient records  $r$ , represented as a series of visits  $V$ , over  $T$  time steps. We represent the  $i$ -th patient record as  $r_i = \{V_1^i, V_2^i, V_3^i, \dots, V_T^i\}$ . Each visit  $V$  also contains several medical codes  $m_1^t, m_2^t, \dots, m_k^t \in C$ , labs  $l_1^t, l_2^t, \dots, l_n^t \in L$  where  $k = |V_C^{(t)}|$  and  $n = |V_L^{(t)}|$ ,  $C$  is the set of medical codes (diagnosis, procedures and medications) and  $L$  is the set of labs. The pipeline allows users to filter the data based on specific criteria and output preprocessed data. The patient records also contain the labels  $D$  for the disease phenotypes as well as static information  $S$  for each patient, where  $S \in \{1, 2, \dots, K\}^N$ , and  $K$  is the number of subgroups.

#### Fairness-Optimized Synthetic Data Generation

The second component of our pipeline is a synthetic EHR data generator. Even though our pipeline is generator agnostic, we have used the HALO EHR generator (represented as  $G$ ) to demonstrate our pipeline. HALO uses a two-module approach: visit-level and code-level. The visit-level module processes a patient’s medical history using transformer decoder blocks, generating visit history representations that summarize the patient’s trajectory. The code-level module generates each variable within a visit based on the patient’s

history and previously generated variables, ensuring intra-visit cohesion. It takes the concatenated visit history embeddings and the preprocessed data  $R$  as input to create a representation of the codes with visit history which is then fed through masked linear layers to model the distribution of each patient code, preserving the autoregressive property. The final output represents the code probabilities used for generating synthetic data.

**Fairness Optimization Objective Function** To make sure that the generator can produce fairness-optimized data, we have implemented a fairness optimization objective function  $\mathcal{L}_F$  in the forward pass of the generator, which ensures that the code probabilities are not biased toward a certain subgroup.

Let us represent the predicted probabilities for each medical code as  $P$ , where  $P \in \mathbb{R}^{N \times T \times C}$ . Let us also denote  $M$  as EHR masks, where  $M \in \{y_1, y_2, \dots\}^{N \times T \times C}$ .

For model loss  $\mathcal{L}(y, \hat{y})$ , we implement the binary cross-entropy (BCE) loss which measures the dissimilarity between the predicted probabilities and the ground truth labels. The general formula for BCE is as follows,

$$\mathcal{L}_{BCE} = -\frac{1}{N} \sum_{i=1}^N \sum_{j=1}^M y_{ij} \log(p_{ij}), \quad (3)$$

where  $N$  is the number of rows and  $M$  is the number of classes. However, in our project, the binary cross entropy loss function works on patient visits and whether a certain medical code exists or not in a certain visit. We can now rewrite equation 2 as the following:

$$\mathcal{L}_{model} = \mathcal{L}_{BCE} + \lambda \mathcal{L}_F \quad (4)$$

The generalized fairness optimization (FO) objective function,  $\mathcal{L}_F$  (Algorithm 1), quantifies the disparity in the predicted probabilities between different subgroups of the sensitive attribute. Based on the fairness task  $F$  the user wants to tackle, it takes the predicted code probabilities  $P$  and the sensitive attribute labels  $S$  as inputs.

Algorithm 1 takes two inputs: the predicted probabilities for each possible outcome ( $P$ ) and the sensitive attribute labels for each instance ( $S$ ). The goal is to compute a fairness loss  $\mathcal{L}_F$  that measures the disparity in the model’s predictions across different subgroups of the sensitive attribute. The fairness objective can be specified by the user based on what type of bias the user plans to address.

The algorithm starts by identifying the unique subgroups  $S_K$  present in the sensitive attribute labels. It then initializes the fairness metric-specific variables that will be used to calculate the fairness loss. These variables may include subgroup-wise statistics, such as sums of predicted probabilities or counts of instances.

Next, the algorithm iterates over the instance  $i$ s, from 1 to  $N$ . For each instance, it retrieves the sensitive attribute subgroup  $s$  and finds the corresponding index  $j$  in the set of unique subgroups  $\mathcal{S}$ . The fairness metric-specific variables are then updated based on the predicted code probabilities  $P_i$ , for instance,  $i$  and its subgroup index  $j$ . This step accumulates the necessary information to compute the fairness

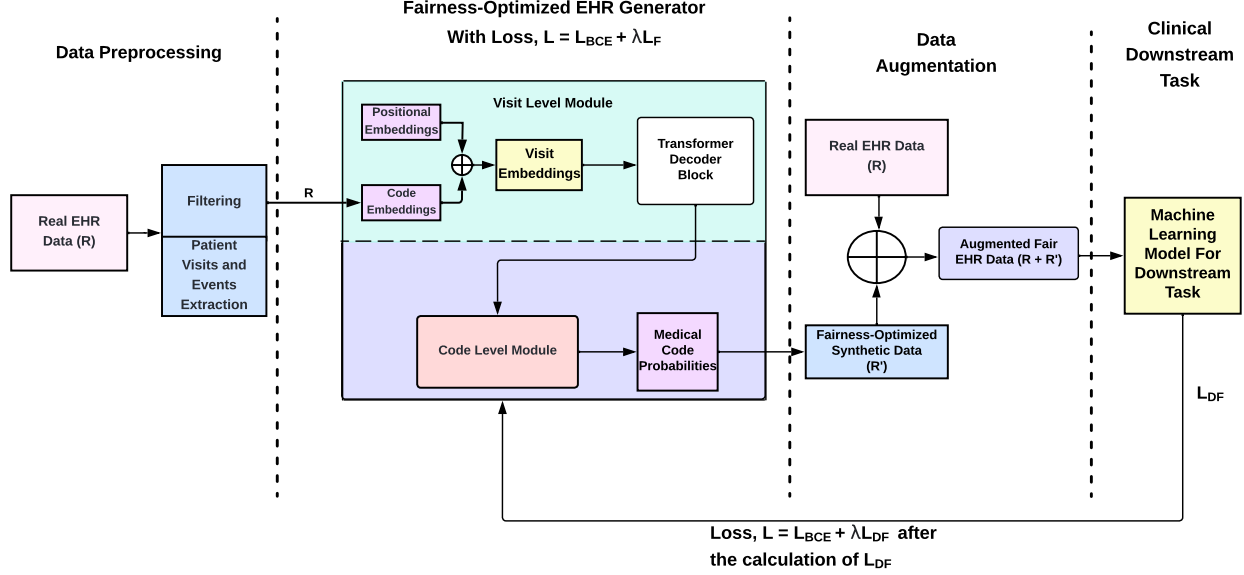


Figure 1: The diagram of our proposed pipeline consists of three major components: data pre-processing, data generation, and data augmentation. The pre-processing stage prepares the EHR data for the generator model alongside any necessary filtering. The generator model generates fair synthetic EHR data. In our project, we have used the HALO model (Theodorou, Xiao, and Sun 2023) with fairness optimization. It has a visit-level module that processes visit embeddings using masked self-attention and a feed-forward network. The output of the self-attention layer and the feed-forward network are normalized (circular blocks) before inputting to the next stage. The code-level module generates each variable within a visit based on the patient’s history and the previously generated variables in the same visit, ensuring maximum intra-visit cohesion (meaning that the generated data should represent a coherent visit where the variables are similar to a typical visit). The loss function of the generator incorporates the proposed fairness objective function or  $\mathcal{L}_F$ . After calculating a fairness metric  $F$  from the downstream task, we feed it back into the loss function as  $\mathcal{L}_{DF}$ .

metric. After processing all instances, the algorithm calculates the fairness metric-specific values using the accumulated information. Finally, the fairness loss  $\mathcal{L}_F$  is calculated based on the fairness metric-specific values which can also be viewed as regularization terms in the model’s overall loss function during training.

We can also input the fairness performance metric of a downstream prediction task (for example, disparate impact in mortality prediction task) into the model loss calculation. We call this value  $\mathcal{L}_{DF}$ . If  $\mathcal{L}_{DF} > 0$ , then the model loss is the sum of  $\mathcal{L}_{BCE}$  and  $\mathcal{L}_{DF}$ . This ensures that the model is optimized directly based on the fairness performance in the specific downstream task of interest. Combining both  $\mathcal{L}_F$  and  $\mathcal{L}_{DF}$  in the calculation of model loss  $\mathcal{L}_{model}$ , we represent the final equation for the loss calculation in 5

$$\mathcal{L}_{model} = \begin{cases} \mathcal{L}_{BCE} + \lambda\mathcal{L}_{DF}, & \text{when } \mathcal{L}_{DF} > 0 \\ \mathcal{L}_{BCE} + \lambda\mathcal{L}_F, & \text{otherwise} \end{cases} \quad (5)$$

The fairness weight  $\lambda$  controls the trade-off between the model’s predictive performance (measured by the BCE loss) and its fairness to the sensitive attribute (measured by the generalized fairness loss).

During training, the model’s parameters are updated to minimize the total loss  $\mathcal{L}$ . This encourages the model to learn to make accurate predictions (by minimizing the BCE loss) while simultaneously reducing the disparity between sensitive attribute subgroups (by minimizing the generalized fairness loss). The goal is to find a balance between predictive performance and fairness, as determined by the fairness weight  $\lambda$ .

### Augmentation of Real Data

After we generate the FO synthetic data  $R'$  and ensure that the real EHR data  $R$  and the FO synthetic data are in the same format, we join both of the datasets to finally obtain  $R + R'$ . This merged pool of real and synthetic data can be then used in the downstream prediction task.

## Experiments

### Data Description

To demonstrate the efficacy of our pipeline, we have performed a set of experiments over two datasets: the MIMIC-III dataset (Johnson et al. 2016) and the PIC (Pediatric Intensive Care) dataset (Zeng et al. 2020). Both of them are available in Physionet data bank (Goldberger et al. 2000). The

---

**Algorithm 1: Fairness Optimization (FO) Objective**

---

**Require:**  $P \in \mathbb{R}^{N \times C}$  - Predicted probabilities for each outcome, where  $N$  is the number of instances and  $C$  is the number of possible outcomes

**Require:**  $S \in 1, 2, \dots, K^N$  - Sensitive attribute labels for each instance, where  $K$  is the number of subgroups

**Require:**  $F$  is fairness objective

**Ensure:**  $\mathcal{L}_F$  - Fairness loss

- 1:  $\mathcal{S} \leftarrow \text{unique}(S)$  {Get the unique sensitive attribute subgroups}
- 2: Initialize fairness metric-specific variables
- 3: **for**  $i \leftarrow 1$  **to**  $N$  **do**
- 4:    $s \leftarrow S_i$  {Get the sensitive attribute subgroup of instance  $i$ }
- 5:    $j \leftarrow \text{index}(s, \mathcal{S})$  {Find the index of the subgroup in  $\mathcal{S}$ }
- 6:   Update fairness metric-specific variables based on  $P_i$  and  $j$
- 7: **end for**
- 8: Calculate fairness metric-specific values
- 9:  $\mathcal{L}_F \leftarrow$  Compute fairness loss based on the fairness metric
- 10: **return**  $\mathcal{L}_F$

---

MIMIC-III dataset is sourced from the Medical Information Mart for Intensive Care (MIMIC), to analyze inpatient records. This extensive dataset encompasses anonymized EHRs originating from patients admitted to the Beth Israel Deaconess Medical Center in Boston, MA, USA, from 2001 to 2012. The data contains information for each patient regarding hospital stay, including laboratory measurements, medications administered, and, vital signs. From the whole dataset, we have used the ICU stay dataset. It contains 46,520 patients with 25 disease phenotype labels which were defined by the MIMIC benchmark (Harutyunyan et al. 2019). Among the patients, 32,950 patients identify as male and the remaining ones identify as females. The dataset has more than 30 ethnicities however to simplify processing, we decided to group the different ethnicities into 5 categories based on the ethnicity names containing White, Black, Hispanic, or Asian keywords. So, the groups are White, Black, Hispanic, Asian, and Others. The White ethnicity has the most samples in the dataset which is 41,325 samples and the rest are of the other groups.

On the other hand, the Pediatric Intensive Care (PIC) database is a large pediatric-specific, single-center, bilingual database comprising information relating to children admitted to critical care units at the Children’s Hospital, Zhejiang University School of Medicine. The dataset has a similar structure to the MIMIC-III dataset however the dataset is smaller having 13,449 patients: 7,728 of whom identify as male and the rest identify as females. Considering the ethnic distribution, it is very skewed toward the Han ethnic group (13,300 patients and the rest of the patient population belongs to the Miao, Tujia, Buyei, Yi, and Hui ethnic groups.

## Data Extraction and Feature Selection

**MIMIC-III dataset:** We worked with the PATIENTS, ADMISSIONS, DIAGNOSES\_ICD, PRESCRIPTIONS, and PROCEDURE\_ICD tables. For each patient, we extracted the time series events, episode-level information (patient age, gender, ethnicity), and patient mortality following the approach explained by Harutyunyan et al. (2019). The dataset contains static data (e.g., gender, ethnicity, diagnosis codes, procedure codes, expiry flag of the patient) and continuous data (e.g., lab results, age). Our cohort from MIMIC-III consists of ICU patients.

**PIC dataset:** From the PIC dataset, we worked with the PATIENTS, ADMISSIONS, and DIAGNOSES\_ICD tables. This dataset only includes children admitted to critical care units and contains static data (e.g., gender, ethnicity, diagnosis codes, expiry flag of the patient) and continuous data (e.g., lab results, age).

In both cases, the continuous data were converted to discrete values using granular discretization, and static data were converted into labels. Finally, for both cohorts, our downstream task is to predict mortality in the next visit of a patient based on the current visit.

## Experimental Methods

We conducted several experiments to explore the efficacy of our proposed pipeline in various scenarios. In our experiments, we have used ‘ethnicity’ as the sensitive attribute. In our pipeline, fairness optimization is facilitated through an FO objective, allowing users to select the specific fairness metric. Throughout our experiments, we utilize DI or disparate impact as the FO objective function (implementation can be found in appendix A.1). DI quantifies the adverse impact of a model’s predictions on a protected group by comparing selection rates between disadvantaged and advantaged groups (Caton and Haas 2024). The ideal value of DI is 1 or near 1. Subsequently, in addition to DI, we assess the fairness of the downstream model using the worst true positive rate (worst TPR or WTPR) which denotes the lowest TPR among all protected groups and underscores the model’s capability to identify positive cases within the most disadvantaged group (Diana et al. 2021). The higher this is, the better the model is identifying true positives for the subgroups.

**Downstream Prediction Model:** Both of these metrics were evaluated on two separate transformer-based prediction models that were trained on multiple subsets of the real dataset and the synthetic dataset. The model’s embedding layer holds the embeddings for input features: visit codes, disease labels, ethnicity, and gender. The final output is a single value denoting whether a patient will be alive in the next hospital visit. The linear layers include separate linear transformations for visit codes, disease labels, ethnicity, and gender. These linear layers project the input features into a common 128-dimensional space.

The core of the model is the transformer component, which contains separate transformer layers for each input feature (visit codes, disease labels, ethnicity, and gender). Each transformer layer consists of a transformer block

that includes a multi-headed attention module for capturing dependencies within the input sequence, and a position-wise feed-forward module for non-linear transformations. The transformer layers also include layer normalization and dropout regularization. The outputs from the transformer layers are concatenated and passed through a final fully connected layer to produce the model’s output, which is a single value. The model is trained using an Adam optimizer with a learning rate of 0.001, no weight decay, and no maximum gradient norm. The batch size is set to 64, and the model is trained for 30 epochs.

The training data were built in two ways: i) augmenting a varying number of real data samples with a fixed number of synthetic samples and ii) augmenting a fixed number of real data samples with a varying number of synthetic samples. The whole dataset was divided into 80-10-10 train-validation-test split.

**Baselines:** Lastly, we compare the performance of the pipeline for the following baselines for both the MIMIC-III and the PIC dataset. For comparison, we designate our method as *Real+FairSynth*. Our tests enable us to assess our proposed pipeline against a variety of baselines that are most pertinent to our group fairness-related work.

- *Real Only* data from the real dataset is used to train the downstream models.
- *Real+Synth* The real data is augmented with synthetic data generated through the HALO generator without the implementation of the FO objective function. This can also be considered as part of the ablation study.
- *Real+Oversample* The real data is over-sampled using the double prioritized bias correction mentioned in the works by Pias et al. (2024). The double prioritized (DP) bias correction method focuses on addressing data imbalance in a specific subgroup, such as a specific ethnicity. It works by incrementally replicating data points of the minority class (diabetes positive) up to n times. In our experiments, we replicated patient data belonging to each minority ethnicity.

**Experiment types** To study the impact of the fairness objective function in fair EHR data generation, we first observe the fairness metrics in the real data. Table 1a compares DI and WTPR for the 3 baselines and our proposed method. In our experiments, we aim to evaluate the impact of the size of the real dataset and the synthetic data set on the fairness and accuracy of the prediction model for fairness weight  $\lambda=1$ .

### Fairness Evaluation in Mortality Prediction with MIMIC-III Dataset

**Experiment 1** Looking at our DI metric for  $\lambda = 1.2$ , our proposed method achieved the best results for 5,000 real samples whereas oversampling the real data achieved better results for a lower number of samples.

Turning to the worst-case TPR metric, where a higher value is better, our proposed method again proves superior. At 1,000 samples, it achieves a TPR of  $0.44 \pm 0.02$ , considerably higher than Real-Only ( $0.48 \pm 0.02$ ), Real+Oversample ( $0.26 \pm 0.01$ ) and Real+Synth ( $0.17 \pm 0.05$ ). The proposed method maintains its lead at larger sample sizes too,

with a TPR of  $0.73 \pm 0.08$  at 5,000 samples compared to  $0.67 \pm 0.06$ ,  $0.14 \pm 0.02$  and  $0.14 \pm 0.02$  for the three baselines respectively.

**Experiment 2** Experiments were conducted where 2,500 real data samples were augmented using a varying number of synthetic samples. Table 1b shows that increasing the number of synthetic samples yields improvements for all methods. However, the proposed Real+FairSynth consistently achieves DI values nearest to the ideal value of 1. At 500 synthetic samples, Real+FairSynth has a DI of  $0.90 \pm 0.07$ . This advantage is maintained at 1,000 and 2000 synthetic samples, with Real+FairSynth reaching an impressive DI of  $0.84 \pm 0.16$  at the 2000 sample mark, compared to  $0.99 \pm 0.06$  and  $1.02 \pm 0.04$  for the other methods.

Turning attention to the worst-case True Positive Rate (WTPR) the results again favor the Real+FairSynth approach as the number of synthetic samples increases. At 500 synthetic samples, Real+FairSynth achieves a WTPR of  $0.65 \pm 0.11$ , outpacing Real+Oversample  $0.16 \pm 0.02$  and Real+Synth  $0.16 \pm 0.04$ . The performance gap widens at 1,000 synthetic samples, with Real+FairSynth reaching  $0.74 \pm 0.13$  versus  $0.15 \pm 0.01$  and  $0.19 \pm 0.03$  for the alternatives. Finally, at 2000 samples, Real+FairSynth demonstrates an impressive WTPR of  $0.77 \pm 0.12$ , substantially higher than Real+Oversample  $0.15$  and Real+Synth  $0.25 \pm 0.01$ . These findings suggest that augmenting a fixed real dataset with an increasing number of synthetic samples can enhance fairness metrics and that the proposed Real+FairSynth method is particularly effective.

### Fairness Evaluation in Mortality Prediction with PIC Dataset

**Experiment 1** Similar to the MIMIC-III dataset, two sets of experiments were run on the PIC dataset: one where a variable number of real samples were augmented with a fixed number of datasets and another one where a fixed size real dataset was augmented with a variable number of synthetic data. It can be observed from Table 2a that our proposed method (Real+FairSynth) consistently achieves the most favorable DI values. For 2,500 and 5,000 data samples, the DI measure was near 1 compared to the other baselines.

Shifting focus to the WTPR, Real+FairSynth demonstrates superior performance across all real sample sizes. With 1,000 real samples, Real+FairSynth achieves a WTPR of  $0.29 \pm 0.09$ , considerably higher than Real-Only ( $0.12 \pm 0.03$ ), Real+Oversample ( $0.08 \pm 0.03$ ), and Real+Synth ( $0.13 \pm 0$ ). For, 5,000 real samples, Real+FairSynth reaches a WTPR of  $0.30 \pm 0.11$ , which is also higher than the alternatives.

Overall, using our proposed method has given us consistently better results compared to the other methods.

**Experiment 2** Table 2b also shows improved results for Real+FairSynth for a variable number of synthetic data samples.

To summarize, the comparative analysis (results are shown in table 1 and 2 provides strong evidence that our proposed methodology outperforms the baselines on both key fairness metrics of DI and WTPR across different ranges

# of Real Samples	Disparate Impact (DI)				WTPR $\uparrow$			
	Real Only	Real+ Oversample	Real+ Synth	Real+ FairSynth	Real Only	Real+ Oversample	Real+ Synth	Real+ FairSynth
<b>1,000</b>	0.98 $\pm$ 0.02	0.99 $\pm$ 0.03	0.97 $\pm$ 0.04	<b>1<math>\pm</math>0.05</b>	0.48 $\pm$ 0.07	0.26 $\pm$ 0.01	0.17 $\pm$ 0.03	<b>0.72<math>\pm</math>0.03</b>
<b>2,500</b>	<b>0.98<math>\pm</math>0.05</b>	0.98 $\pm$ 0.04	0.97 $\pm$ 0.04	1.28 $\pm$ 0.42	0.51 $\pm$ 0.06	0.2 $\pm$ 0.007	0.17 $\pm$ 0.01	<b>0.72<math>\pm</math>0.02</b>
<b>5,000</b>	0.99 $\pm$ 0.02	0.99 $\pm$ 0.02	0.98 $\pm$ 0.03	<b>0.99<math>\pm</math>0.16</b>	0.67 $\pm$ 0.06	0.14 $\pm$ 0.02	0.14 $\pm$ 0.02	<b>0.73<math>\pm</math>0.08</b>

(a) Fairness metrics for Experiment 1

# of Synthetic Samples	Disparate Impact (DI)			WTPR $\uparrow$		
	Real+ Oversample	Real+ Synth	Real+ FairSynth	Real+ Oversample	Real+ Synth	Real+ FairSynth
<b>500</b>	0.98 $\pm$ 0.03	0.98 $\pm$ 0.04	<b>0.98<math>\pm</math>0.22</b>	0.16 $\pm$ 0.04	0.16 $\pm$ 0.02	<b>0.24<math>\pm</math>0.14</b>
<b>1,000</b>	<b>0.99<math>\pm</math>0.03</b>	0.98 $\pm$ 0.02	1.28 $\pm$ 0.42	0.19 $\pm$ 0.03	0.15 $\pm$ 0.01	<b>0.72<math>\pm</math>0.02</b>
<b>2,000</b>	1.02 $\pm$ 0.04	0.99 $\pm$ 0.06	<b>1.03<math>\pm</math>0.44</b>	0.25 $\pm$ 0.01	0.15 $\pm$ 0	<b>0.83<math>\pm</math> 0.06</b>

(b) Fairness metrics for Experiment 2

Table 1: Comparison of the fairness metrics between the baselines and our proposed pipeline for the MIMIC-III dataset. Table 1a shows the metrics we received from Experiment 1 where a variable number of real data samples and a fixed number of synthetic samples (2,500 samples) were used. Experiment 2’s results are shown in table 1b where a variable number of synthetic data samples and a fixed number of real samples (2,500 samples) were used. Here the bold numbers are the values close to ideal values. Mean  $\pm$  standard deviation.  $\uparrow$ : Higher is better

# of Real Samples	Disparate Impact (DI)				WTPR $\uparrow$			
	Real Only	Real+ Oversample	Real+ Synth	Real+ FairSynth	Real Only	Real+ Oversample	Real+ Synth	Real+ FairSynth
<b>1,000</b>	0.87 $\pm$ 0.51	1.41 $\pm$ 0.81	0.42 $\pm$ 0	<b>0.66<math>\pm</math>0.23</b>	0.12 $\pm$ 0.03	0.08 $\pm$ 0.03	0.13 $\pm$ 0	<b>0.29<math>\pm</math>0.09</b>
<b>2,500</b>	0.39 $\pm$ 0.49	1.38 $\pm$ 0.32	<b>0.85<math>\pm</math>0.15</b>	1.35 $\pm$ 0.61	0.06 $\pm$ 0.05	0.1 $\pm$ 0.04	<b>0.27<math>\pm</math>0.16</b>	0.23 $\pm$ 0.15
<b>5,000</b>	0.76 $\pm$ 0.77	0.95 $\pm$ 0.18	1.11 $\pm$ 0.76	<b>1.09<math>\pm</math>0.29</b>	0.05 $\pm$ 0.02	0.15 $\pm$ 0.13	0.19 $\pm$ 0.17	<b>0.30<math>\pm</math>0.11</b>

(a) Fairness metrics for Experiment 1

# of Synthetic Samples	Disparate Impact (DI)			WTPR $\uparrow$		
	Real+ Oversample	Real+ Synth	Real+ FairSynth	Real+ Oversample	Real+ Synth	Real+ FairSynth
<b>500</b>	1.34 $\pm$ 0.44	1.3 $\pm$ 0.52	<b>1.30<math>\pm</math>0.52</b>	0.06 $\pm$ 0.03	0.1 $\pm$ 0.6	<b>0.1<math>\pm</math>0.06</b>
<b>1,000</b>	<b>1.27<math>\pm</math>0.3</b>	1.65 $\pm$ 0.62	1.35 $\pm$ 0.61	0.13 $\pm$ 0.11	0.04 $\pm$ 0.01	<b>0.4<math>\pm</math>0.01</b>
<b>2,000</b>	0.76 $\pm$ 0.65	0.64 $\pm$ 0	<b>0.64<math>\pm</math>0</b>	0.05 $\pm$ 0.02	0.02 $\pm$ 0	<b>0.02<math>\pm</math>0</b>

(b) Fairness metrics for Experiment 2

Table 2: Comparison of the fairness metrics between the baselines and our proposed pipeline for the PIC dataset. Table 2a shows the metrics we received for a variable number of real data samples and a fixed number of synthetic samples (2,500 samples). Table 2b shows the same metrics for a variable number of synthetic data samples and a fixed number of real samples (2,500 samples). Here the bold numbers are the values close to ideal values: for DI, closer to 1 is better, and for WTPR, higher is better. Mean  $\pm$  standard deviation.  $\uparrow$ : Higher is better

of sample sizes evaluated. This also shows that, even with a few real samples, adding synthetic samples generated by our proposed method can improve the fairness metrics.

### Prediction Performance

We have also observed the prediction performance of the transformer-based model alongside the fairness metrics for the baseline datasets and the Real+FairSynth. The prediction performance is measured using the F1-score. From table 3, we can observe, the f1-scores for the real data and augmented datasets for different numbers of real and synthetic samples. It can be observed that, for both MIMIC-III and PIC datasets, augmenting the data with our proposed fairness-optimized synthetic data does not increase the predictive performance compared to the other dataset which showcases the trade-off between prediction performance and fairness.

### Trade-off Between Fairness and Prediction Accuracy

In this study, we investigate the trade-off between prediction performance and fairness metrics by varying the value of the fairness weight parameter,  $\lambda$ . This analysis is crucial in understanding how different values of  $\lambda$  impact both the F1-scores and fairness metrics such as Disparate Impact (DI) and Weighted True Positive Rate (WTPR).

**Impact on Prediction Performance** Table 4a illustrates the F1-scores for different values of  $\lambda$  on the MIMIC-III dataset across three different sample sizes (1000, 2500, and 5000). As  $\lambda$  increases from 0.5 to 1.5, there is a noticeable decline in the F1 scores. For example, for 5000 samples, the F1-score reduces from  $0.46 \pm 0.02$  at  $\lambda = 0.5$  to  $0.24 \pm 0.02$  at  $\lambda = 1.5$ . This trend clearly shows that higher values of  $\lambda$  negatively impact the prediction performance, as the declining F1 scores indicate.

**Impact on Fairness Metrics** Conversely, Table 4b presents the DI and WTPR values for the same variations in  $\lambda$  and sample sizes. Here, a higher value of  $\lambda$  generally enhances the fairness metrics. However, we observe that increasing the  $\lambda$  too much, for example, from 1.2 to 1.5, affects the DI impact positively but WTPR negatively indicating that, changing the lambda value causes variation in the fairness metrics.

In summary, we have observed a trade-off between accuracy (F1-scores) and fairness (DI and WTPR) metrics is a crucial aspect of model optimization. Lower values of  $\lambda$  prioritize prediction performance, resulting in higher F1 scores but potentially less fair outcomes. In contrast, higher values of  $\lambda$  improve fairness metrics at the expense of prediction accuracy.

This trade-off suggests that the specific goals of the application should guide the choice of  $\lambda$ . If the priority is to maximize prediction accuracy, lower values of  $\lambda$  may be preferable. However, if fairness is a critical objective, higher values of  $\lambda$  should be considered despite the associated decrease in prediction performance. Balancing this trade-off is key to developing models that are both effective and fair,

tailored to the ethical and operational requirements of the specific use case.

### Limitations

Our proposed pipeline has several limitations. Firstly, while our pipeline in the current version is limited to tabular data, it still establishes a valuable foundation for generating fairness-optimized synthetic data and has shown good results. Including other modalities like medical images or medical notes in future versions might improve the output of the pipeline. Secondly, due to limited computing resources, we were not able to train the generator models and the downstream prediction models longer. We expect that running the models for a longer time would improve the quality of the output even further. Finally, our current version of the pipeline supports augmentation as the sole debiasing method. We plan to include other debiasing methods in future versions.

### Conclusion

In this study, we presented a pipeline for generating on-demand fairness-optimized synthetic electronic health record data that can pre-process the data for feeding into an EHR generator and augment real data with fairness-optimized (FO) synthetic data. Specifically, we used FO objective function to ensure that combining the real data with the generated synthetic data can improve the fairness performance of downstream predictive models running on the data. Through a series of comprehensive experiments on MIMIC-III and pediatric ICU datasets, we showed that the addition of FO objectives in the generator and augmenting real data with FO synthetic data can indeed reduce the biases observed for different sensitive attributes in downstream mortality prediction tasks. Even though our method solely focuses on data-related methods where we try to improve fairness by augmenting, it is possible to combine our proposed method with model-related techniques (where the downstream model is modified) and inference-related techniques (where post-processing is performed on the output). Our model can also be extended by implementing objective functions to incorporate multi-label sensitive attributes and multi-modal debiasing.

### Acknowledgments

Our study was partially supported by NIH awards, P20GM103446 and P20GM113125, and a gift from Amazon Web Services.

### References

- Baowaly, M. K.; Lin, C.-C.; Liu, C.-L.; and Chen, K.-T. 2019. Synthesizing electronic health records using improved generative adversarial networks. *Journal of the American Medical Informatics Association*, 26(3): 228–241.
- Bhanot, K.; Baldini, I.; Wei, D.; Zeng, J.; and Bennett, K. P. 2022. Downstream Fairness Caveats with Synthetic Healthcare Data. *arXiv preprint arXiv:2203.04462*.
- Caton, S.; and Haas, C. 2024. Fairness in Machine Learning: A Survey. *ACM Comput. Surv.*, 56(7).



F1-Score For Mortality Prediction (MIMIC-III) <sup>†</sup>								
# of Real Samples	Real Only	Real + Oversample	Real+ Synth	Real+ FairSynth	# of Synthetic Samples	Real + Oversample	Real+ Synth	Real+ FairSynth
1,000	<b>0.53±0.06</b>	0.27±0.09	0.25±0.03	0.33±0.13	500	0.27±0.03	0.25±0.05	<b>0.33±0.06</b>
2,500	<b>0.51±0.09</b>	0.28±0.07	0.27±0.06	0.29±0.11	1,000	<b>0.29±0.03</b>	0.26±0.04	0.22±0.05
5,000	<b>0.55±0.03</b>	0.28±0.06	0.27±0.05	0.26±0.14	2,500	0.33±0.02	0.26±0.04	<b>0.34±0.05</b>

(a)

F1-Score For Mortality Prediction (PIC Dataset)								
# of Real Samples	Real Only	Real + Oversample	Real+ Synth	Real+ FairSynth	# of Synthetic Samples	Real + Oversample	Real+ Synth	Real+ FairSynth
1,000	0.38±0.25	<b>0.62±0.02</b>	0.14±0.12	0.1±0.09	500	<b>0.56±0.07</b>	0.51±0.17	0.11±0.03
2,500	0.36±0.25	<b>0.6±0.05</b>	0.12±0.06	0.13±0.09	1,000	<b>0.57±0.06</b>	0.45±0.02	0.1±0.04
5,000	0.35±0.25	<b>0.57±0.01</b>	0.09±0.05	0.13±0.03	2,500	<b>0.58±0.05</b>	0.41±0.02	0.1±0.05

(b)

Table 3: F1-scores for next-visit mortality prediction tasks for augmented datasets created from the two datasets. Table 3a shows the F1-scores for the MIMIC-III dataset and table 3b shows the F1-scores for the PIC dataset. Mean±Standard Deviation. <sup>†</sup>: Higher is Better

Ceritli, T.; Ghosheh, G. O.; Chauhan, V. K.; Zhu, T.; Creagh, A. P.; and Clifton, D. A. 2023. Synthesizing mixed-type electronic health records using diffusion models. *arXiv preprint arXiv:2302.14679*.

Che, Z.; and Liu, Y. 2017. Deep learning solutions to computational phenotyping in health care. In *2017 IEEE International Conference on Data Mining Workshops (ICDMW)*, 1100–1109. IEEE.

Choi, E.; Bahadori, M. T.; Song, L.; Stewart, W. F.; and Sun, J. 2017a. GRAM: graph-based attention model for healthcare representation learning. In *Proceedings of the 23rd ACM SIGKDD international conference on knowledge discovery and data mining*, 787–795.

Choi, E.; Bahadori, M. T.; Sun, J.; Kulas, J.; Schuetz, A.; and Stewart, W. 2016. Retain: An interpretable predictive model for healthcare using reverse time attention mechanism. *Advances in neural information processing systems*, 29.

Choi, E.; Biswal, S.; Malin, B.; Duke, J.; Stewart, W. F.; and Sun, J. 2017b. Generating multi-label discrete patient records using generative adversarial networks. In *Machine learning for healthcare conference*, 286–305. PMLR.

Chouldechova, A.; and Roth, A. 2018. The frontiers of fairness in machine learning. *arXiv preprint arXiv:1810.08810*.

Cui, L.; Biswal, S.; Glass, L. M.; Lever, G.; Sun, J.; and Xiao, C. 2020. CONAN: complementary pattern augmentation for rare disease detection. In *Proceedings of the AAAI Conference on Artificial Intelligence*, volume 34, 614–621.

Devlin, J.; Chang, M.-W.; Lee, K.; and Toutanova, K. 2018.

Bert: Pre-training of deep bidirectional transformers for language understanding. *arXiv preprint arXiv:1810.04805*.

Diana, E.; Gill, W.; Kearns, M.; Kenthapadi, K.; and Roth, A. 2021. Minimax group fairness: Algorithms and experiments. In *Proceedings of the 2021 AAAI/ACM Conference on AI, Ethics, and Society*, 66–76.

Dwork, C.; Hardt, M.; Pitassi, T.; Reingold, O.; and Zemel, R. 2012. Fairness through awareness. In *Proceedings of the 3rd innovations in theoretical computer science conference*, 214–226.

Fu, T.; Hoang, T. N.; Xiao, C.; and Sun, J. 2019. Ddl: Deep dictionary learning for predictive phenotyping. In *IJCAI: proceedings of the conference*, volume 2019, 5857. NIH Public Access.

Goldberger, A. L.; Amaral, L. A.; Glass, L.; Hausdorff, J. M.; Ivanov, P. C.; Mark, R. G.; Mietus, J. E.; Moody, G. B.; Peng, C.-K.; and Stanley, H. E. 2000. PhysioBank, PhysioToolkit, and PhysioNet: components of a new research resource for complex physiologic signals. *circulation*, 101(23): e215–e220.

Goodfellow, I.; Pouget-Abadie, J.; Mirza, M.; Xu, B.; Warde-Farley, D.; Ozair, S.; Courville, A.; and Bengio, Y. 2014. Generative adversarial nets. *Advances in neural information processing systems*, 27.

Gupta, M.; Phan, T.-L. T.; Bunnell, H. T.; and Beheshti, R. 2022. Obesity Prediction with EHR Data: A Deep Learning Approach with Interpretable Elements. *ACM Trans. Comput. Healthcare*, 3(3).

# of Real Samples	F1-scores for different values of $\lambda$ for MIMIC-III dataset $\uparrow$			
	$\lambda = 0.5$	$\lambda = 1$	$\lambda = 1.2$	$\lambda = 1.5$
<b>1000</b>	<b>0.55±0.03</b>	0.1±0.09	0.45±0.02	0.22±0.08
<b>2500</b>	<b>0.52±0.02</b>	0.13±0.09	0.49±0.01	0.24±0.01
<b>5000</b>	<b>0.46±0.02</b>	0.13±0.025	0.45±0.03	0.24±0.02

(a) F1-scores for different values of fairness weight,  $\lambda$ 

# of Real Samples	DI and WTPR for different values of $\lambda$ for MIMIC-III dataset							
	$\lambda = 0.5$	$\lambda = 1$	$\lambda = 1.2$	$\lambda = 1.5$	$\lambda = 0.5$	$\lambda = 1$	$\lambda = 1.2$	$\lambda = 1.5$
<b>1000</b>	1.28±1.21	1±0.05	0.89±0.66	<b>1.00±0.06</b>	0.64±0.24	<b>0.72±0.03</b>	0.44±0.23	0.15±0.08
<b>2500</b>	0.99±0.22	1.28±0.42	1.20±0.28	<b>0.99±0.02</b>	0.74±0.09	0.72±0.02	<b>0.75±0.05</b>	0.15±0.01
<b>5000</b>	1.10±0.09	0.99±0.16	1.10±0.09	<b>0.99±0.04</b>	0.78±0.07	0.73±0.08	<b>0.78±0.07</b>	0.15±0.02

(b) DI and WTPR values for different values of fairness weight,  $\lambda$ 

Table 4: Effect of changing  $\lambda$  values on F1-score and fairness metrics. We can observe that we get a higher f1-score for lower  $\lambda$  values showing better prediction performance by trading off fairness. On the other hand, in table 4b, we get better fairness scores for higher values of  $\lambda$ , 1, 1.2.

. Mean±standard Deviation  $\uparrow$ : Higher is better

Harutyunyan, H.; Khachatrian, H.; Kale, D. C.; Ver Steeg, G.; and Galstyan, A. 2019. Multitask learning and benchmarking with clinical time series data. *Scientific data*, 6(1): 96.

He, H.; Zhao, S.; Xi, Y.; and Ho, J. C. 2023. MedDiff: Generating electronic health records using accelerated denoising diffusion model. *arXiv preprint arXiv:2302.04355*.

Johnson, A. E. W.; Pollard, T. J.; Shen, L.; Lehman, L.-W. H.; Feng, M.; Ghassemi, M.; Moody, B.; Szolovits, P.; Celi, L. A.; and Mark, R. G. 2016. MIMIC-III, a freely accessible critical care database. *Scientific data*, 3(1): 1–9.

Li, J.; Cairns, B. J.; Li, J.; and Zhu, T. 2023. Generating synthetic mixed-type longitudinal electronic health records for artificial intelligent applications. *NPJ Digital Medicine*, 6(1): 98.

Moore, W.; and Frye, S. 2020. Review of HIPAA, Part 2: Limitations, Rights, Violations, and Role for the Imaging Technologist. *Journal of Nuclear Medicine Technology*, 48(1): 17–23.

Mottalib, M. M.; Jones-Smith, J. C.; Sheridan, B.; and Beheshti, R. 2023. Subtyping Patients With Chronic Disease Using Longitudinal BMI Patterns. *IEEE Journal of Biomedical and Health Informatics*, 27(4): 2083–2093.

Narayanan, A. 2018. Translation tutorial: 21 fairness definitions and their politics. In *Proc. conf. fairness accountability transp., new york, usa*, volume 1170, 3.

Pang, C.; Jiang, X.; Pavinkurve, N. P.; Kalluri, K. S.; Minto, E. L.; Patterson, J.; Zhang, L.; Hripcsak, G.; Elhadad, N.; and Natarajan, K. 2024. CEHR-GPT: Generating Electronic Health Records with Chronological Patient Timelines. *arXiv:2402.04400*.

Pias, T. S.; Su, Y.; Tang, X.; Wang, H.; Faghani, S.; and Yao, D. D. 2024. Enhancing Fairness and Accuracy in Diagnosing Type 2 Diabetes in Young Population. *medRxiv*.

Poulain, R.; Bin Tarek, M. F.; and Beheshti, R. 2023. Improving Fairness in AI Models on Electronic Health Records: The Case for Federated Learning Methods. In *Proceedings of the 2023 ACM Conference on Fairness, Accountability, and Transparency*, FAccT '23, 1599–1608. New York, NY, USA: Association for Computing Machinery. ISBN 9798400701924.

Poulain, R.; Gupta, M.; and Beheshti, R. 2022. Few-Shot Learning with Semi-Supervised Transformers for Electronic Health Records. In *Proceedings of the Machine Learning for Healthcare (MLHC-2022)*.

Poulain, R.; Gupta, M.; Foraker, R.; and Beheshti, R. 2021. Transformer-based Multi-target Regression on Electronic Health Records for Primordial Prevention of Cardiovascular Disease. In *2021 IEEE International Conference on Bioinformatics and Biomedicine (BIBM)*, 726–731.

Radford, A.; Wu, J.; Child, R.; Luan, D.; Amodei, D.; Sutskever, I.; et al. 2019. Language models are unsupervised multitask learners. *OpenAI blog*, 1(8): 9.

Ramazi, R.; Perndorfer, C.; Soriano, E.; Laurenceau, J.-P.; and Beheshti, R. 2019. Multi-Modal Predictive Models of Diabetes Progression. In *Proceedings of the 10th ACM International Conference on Bioinformatics, Computational Biology and Health Informatics*, 253–258. New York, NY, USA: Association for Computing Machinery. ISBN 9781450366663.

Ras, G.; Xie, N.; Van Gerven, M.; and Doran, D. 2022. Explainable deep learning: A field guide for the uninitiated. *Journal of Artificial Intelligence Research*, 73: 329–396.

Rashidian, S.; Wang, F.; Moffitt, R.; Garcia, V.; Dutt, A.; Chang, W.; Pandya, V.; Hajagos, J.; Saltz, M.; and Saltz, J. 2020. SMOOTH-GAN: towards sharp and smooth synthetic EHR data generation. In *Artificial Intelligence in Medicine: 18th International Conference on Artificial Intelligence in Medicine, AIME 2020, Minneapolis, MN, USA, August 25–28, 2020, Proceedings 18*, 37–48. Springer.

Shang, J.; Ma, T.; Xiao, C.; and Sun, J. 2019a. Pre-training of graph augmented transformers for medication recommendation. *arXiv preprint arXiv:1906.00346*.

Shang, J.; Xiao, C.; Ma, T.; Li, H.; and Sun, J. 2019b. Gamenet: Graph augmented memory networks for recommending medication combination. In *proceedings of the AAAI Conference on Artificial Intelligence*, volume 33, 1126–1133.

Sun, S.; Wang, F.; Rashidian, S.; Kurc, T.; Abell-Hart, K.; Hajagos, J.; Zhu, W.; Saltz, M.; and Saltz, J. 2021. Generating longitudinal synthetic ehr data with recurrent autoencoders and generative adversarial networks. In *Heterogeneous Data Management, Polystores, and Analytics for Healthcare: VLDB Workshops, Poly 2021 and DMAH 2021, Virtual Event, August 20, 2021, Revised Selected Papers 7*, 153–165. Springer.

Theodorou, B.; Xiao, C.; and Sun, J. 2023. Synthesize high-dimensional longitudinal electronic health records via hierarchical autoregressive language model. *Nature Communications*, 14(1): 5305.

Torfi, A.; and Fox, E. A. 2020. CorGAN: correlation-capturing convolutional generative adversarial networks for generating synthetic healthcare records. *arXiv preprint arXiv:2001.09346*.

Touvron, H.; Lavril, T.; Izacard, G.; Martinet, X.; Lachaux, M.-A.; Lacroix, T.; Rozière, B.; Goyal, N.; Hambro, E.; Azhar, F.; et al. 2023. Llama: Open and efficient foundation language models. *arXiv preprint arXiv:2302.13971*.

Vaswani, A.; Shazeer, N.; Parmar, N.; Uszkoreit, J.; Jones, L.; Gomez, A. N.; Kaiser, Ł.; and Polosukhin, I. 2017. Attention is all you need. *Advances in neural information processing systems*, 30.

Voigt, P.; and von dem Bussche, A. 2017. *Introduction and ‘Checklist’*, 1–7. Cham: Springer International Publishing. ISBN 978-3-319-57959-7.

Wang, L.; Zhang, W.; He, X.; and Zha, H. 2018. Supervised reinforcement learning with recurrent neural network for dynamic treatment recommendation. In *Proceedings of the 24th ACM SIGKDD international conference on knowledge discovery & data mining*, 2447–2456.

Xu, D.; Yuan, S.; Zhang, L.; and Wu, X. 2018. Fairgan: Fairness-aware generative adversarial networks. In *2018 IEEE International Conference on Big Data (Big Data)*, 570–575. IEEE.

Yan, C.; Zhang, Z.; Nyemba, S.; and Malin, B. A. 2020. Generating electronic health records with multiple data types and constraints. In *AMIA annual symposium proceedings*, volume 2020, 1335. American Medical Informatics Association.

Zeng, X.; Yu, G.; Lu, Y.; Tan, L.; Wu, X.; Shi, S.; Duan, H.; Shu, Q.; and Li, H. 2020. PIC, a paediatric-specific intensive care database. *Scientific data*, 7(1): 14.

Zhang, Z.; Yan, C.; Lasko, T. A.; Sun, J.; and Malin, B. A. 2021. SynTEG: a framework for temporal structured electronic health data simulation. *Journal of the American Medical Informatics Association*, 28(3): 596–604.

Zhang, Z.; Yan, C.; Mesa, D. A.; Sun, J.; and Malin, B. A. 2020. Ensuring electronic medical record simulation through better training, modeling, and evaluation. *Journal of the American Medical Informatics Association*, 27(1): 99–108.

## A. Appendix

### A.1 Description of the FO Objective Functions Used in Experiments

**Disparate impact** examines the likelihood of receiving a positive classification. However, instead of focusing on the difference between unprivileged and privileged groups, it considers the ratio of these probabilities. The concept of disparate impact has roots in legal fairness assessments for selection processes, where the 80% rule is sometimes applied to determine whether a process exhibits disparate impact (ratio below 0.8) or not (Caton and Haas 2024). We can formalize DI as follows:

Let  $SR_p$  be the selection rate for the protected group,  $SR_n$  be the selection rate for the non-protected group. The selection rate for a group is calculated as the number of favorable outcomes (e.g., positive predictions, approvals) divided by the total number of instances in that group.

So, the disparate impact ratio is  $DI$  then calculated as:

$$DI = \frac{SR_p}{SR_n} \quad (6)$$

The implementation is shown in algorithm 2.

The loss function inputs the predicted probabilities for each code ( $P$ ) and the sensitive attribute labels for each patient ( $G$ ). It first identifies the unique sensitive attribute labels present in the dataset ( $\mathcal{G}$ ). Then, it initializes two arrays,  $S_g$  and  $N_g$ , to store the sum of positive predictions and the count of patients for each sensitive attribute group, respectively.

The algorithm then iterates over each patient  $i$  and determines their subgroup  $g$ . It finds the corresponding index  $j$  of the sensitive attribute in the unique label  $\mathcal{G}$ . For each patient, the function counts the number of positive predictions ( $p_i$ ) by summing the indicator function  $\mathbf{1}(P_{i,c} > 0.5)$  over all codes  $c$ . This indicator function returns 1 if the predicted probability  $P_{i,c}$  is greater than 0.5 (i.e., a positive prediction) and 0 otherwise. The count of positive predictions is added to the corresponding sensitive attribute’s sum  $S_{g_j}$ , and the patient count for that sensitive attribute  $N_{g_j}$  is incremented.

After processing all patients, each subgroup’s positive prediction rate  $R_g$  is calculated by dividing the sum of positive predictions  $S_g$  by the patient count  $N_g$  for each gender  $g$ . The disparate impact ratio  $DI$  is then computed as the

---

**Algorithm 2: Disparate Impact Loss Function**

---

**Require:**  $P \in \mathbb{R}^{N \times C}$  - Predicted probabilities for each code, where  $N$  is the number of patients and  $C$  is the number of codes

**Require:**  $G \in 0 \dots N^N$  - {Subgroup labels for a sensitive attribute}

**Ensure:**  $\mathcal{L}_{DI}$  - Disparate impact loss

- 1:  $\mathcal{G} \leftarrow \text{unique}(G)$  {Get the unique subgroup labels}
- 2:  $S_g \leftarrow 0^{|\mathcal{G}|}$  {Initialize sensitive attribute-wise positive prediction sums}
- 3:  $N_g \leftarrow 0^{|\mathcal{G}|}$  {Initialize sensitive attribute-wise patient counts}
- 4: **for**  $i \leftarrow 1$  **to**  $N$  **do**
- 5:    $g \leftarrow G_i$  {Get the sensitive attribute value of patient  $i$ }
- 6:    $j \leftarrow \text{index}(g, \mathcal{G})$  {Find the index of the sensitive attribute in  $\mathcal{G}$ }
- 7:    $p_i \leftarrow \sum_{c=1}^C \mathbf{1}(P_{i,c} > 0.5)$  {Count positive predictions for patient  $i$ }
- 8:    $S_{g_j} \leftarrow S_{g_j} + p_i$  {Add positive prediction count to the corresponding value of the sensitive attribute}
- 9:    $N_{g_j} \leftarrow N_{g_j} + 1$  {Increment the count for the corresponding sub group}
- 10: **end for**
- 11:  $R_g \leftarrow \frac{S_g}{N_g}, \forall g \in \mathcal{G}$  {Calculate the positive prediction rate for each sub group}
- 12:  $DI \leftarrow \frac{R_{g_0}}{R_{g_1}}$  {Compute the disparate impact ratio}
- 13:  $\mathcal{L}_{DI} \leftarrow |1 - DI|$  {Calculate the disparate impact loss}
- 14: **return**  $\mathcal{L}_{DI}$

---

ratio of the positive prediction rates between the subgroups groups.

Finally, the disparate impact loss  $\mathcal{L}_{DI}$  is calculated as the absolute difference between 1 and the disparate impact ratio  $DI$ . This loss function quantifies the deviation from perfect equality (i.e., a disparate impact ratio of 1) between the gender groups. A higher loss value indicates a larger disparate impact, while a lower loss value suggests a more balanced and fair model.

**Worst performing TPR (the lowest) or the Worst TPR.**

It is a useful fairness metric because it focuses on the model’s performance for the most disadvantaged subgroup. It helps identify if there are significant disparities in the model’s performance across different subgroups defined by the protected attribute. Suppose  $A \in [[1, N]]$ , where  $A$  is a categorical sensitive attribute with  $N$  possible values (e.g. gender, race, ethnicity, religion),  $Y \in [0, 1]$  and  $\hat{Y} \in [0, 1]$  as the ground truth and the prediction of a binary predictor, respectively.

$$\text{Worst-Case TPR} = \min_{n \in E} Pr(\hat{Y} = 1 | A = n, Y = 1) \quad (7)$$

A smaller value (closer to zero) is ideal for the parity-based measures, but for the worst TPR, a greater value (closer to one) is desired.

## A.2 Experimental Setup

We split the data into an 80-10-10 ratio for training, validation, and testing. Due to limited computing resources and GPU power, we ran the synthetic EHR generator using the Adam optimizer with a batch size of 10, a sample batch size of 25, and a learning rate of  $10^{-4}$ .

All of our experiments were run using the built-in ML models, specifically a transformer-based model, from the PyHealth library. These models utilize static data, such as demographic information like gender and ethnicity, and continuous time-series data.

The experiments were performed on three environments: Two Windows PCs and in the cloud using Google Colab. The first machine had an Intel Core i9-9900K processor, 32 GB of RAM, and an NVIDIA GeForce RTX 2080Ti GPU with 12GB memory. The second machine featured an Intel Core i9-13900HX processor, 32 GB of RAM, and an NVIDIA GeForce RTX 4070 GPU with 8GB memory. In Google Colab, we utilized the T4, L4, and A100 GPUs. All the codes were run using Python version 3.11.5, CUDA version 12.1, and PyTorch 2.1.2.